LUND UNIVERSITY

The cysteine 34 residue of A1M/α1-microglobulin is essential for protection of irradiated cell cultures and reduction of carbonyl groups.

Rutardottir, Sigurbjörg; Nilsson, E J C; Pallon, Jan; Gram, Magnus; Åkerström, Bo

Published in:
Free Radical Research

DOI:
10.3109/10715762.2013.801555

2013

Link to publication

Citation for published version (APA):
Rutardottir, S., Nilsson, E. J. C., Pallon, J., Gram, M., & Åkerström, B. (2013). The cysteine 34 residue of A1M/α1-microglobulin is essential for protection of irradiated cell cultures and reduction of carbonyl groups. *Free Radical Research*, *47*(6-7), 541-550. https://doi.org/10.3109/10715762.2013.801555

Total number of authors:
5

General rights
Unless other specific re-use rights are stated the following general rights apply:
Copyright and moral rights for the publications made accessible in the public portal are retained by the authors and/or other copyright owners and it is a condition of accessing publications that users recognise and abide by the legal requirements associated with these rights.
• Users may download and print one copy of any publication from the public portal for the purpose of private study or research.
• You may not further distribute the material or use it for any profit-making activity or commercial gain
• You may freely distribute the URL identifying the publication in the public portal

Read more about Creative commons licenses: https://creativecommons.org/licenses/

Take down policy
If you believe that this document breaches copyright please contact us providing details, and we will remove access to the work immediately and investigate your claim.

LUND UNIVERSITY

PO Box 117
221 00 Lund
+46 46-222 00 00

Download date: 04. May. 2026

Original Research Communication

The cysteine 34 residue of A1M/α_1-microglobulin is essential for protection of irradiated cell cultures and reduction of carbonyl groups

Sigurbjörg Rutardottir[1], E.J. Charlotta Nilsson[2], Jan Pallon[2], Magnus Gram[1] and Bo Åkerström[1*]

Divisions of [1]Infection Medicine and [2]Nuclear Physics, Lund University, Lund, Sweden

* To whom correspondence should be addressed:

Bo Åkerström, Division of Infection Medicine, Department of Clinical Sciences in Lund, Lund University, BMC B14, 221 84 Lund, Sweden.

E-mail: bo.akerstrom@med.lu.se; Tel. Nr: +46 46 222 8578; Fax Nr: +46 46 157756

Running title: C34 is essential for A1Ms protection mechanism

Key words: Antioxidant, free radicals, radical scavenging, oxidative stress, alpha particle radiation.

Formatted: German (Germany)

Field Code Changed

Formatted: German (Germany)

Formatted: German (Germany)

ABSTRACT

α_1-microglobulin (A1M) is a 26 kDa plasma and tissue protein belonging to the lipocalin family. The reductase and free radical scavenger A1M has been shown to protect cells and extracellular matrix against oxidative and irradiation-induced damage. The reductase activity was previously shown to depend upon an unpaired cysteinyl side-chain, C34, and three lysyl side-chains, K92, 118 and 130, located around the open end of the lipocalin pocket. The aim of this work was to investigate whether the cell and matrix protection by A1M is a result of its reductase activity by using A1M-variants with site-directed mutations of the C34, K92, K118 and K130 positions. The results show that the C34 side-chain is an absolute requirement for protection of HepG2 cell cultures against alpha-particle irradiation-induced cell death, upregulation of stress response and cell cycle regulation genes. Mutation of C34 also resulted in loss of the reduction capacity towards heme- and hydrogen peroxide-oxidized collagen, and the radical species 2,2´-azino-bis (3-ethyl-benzo-thiazoline-6-sulphonic acid) (ABTS). Furthermore, mutation of C34, significantly suppressed the cell-uptake of A1M. The K92, K118 and K130 side chains were of minor importance in cell protection and reduction of oxidized collagen but strongly influenced the reduction of the ABTS-radical. It is concluded that antioxidative protection of cells and collagen by A1M is totally dependent on its C34 amino acid residue. A model of the cell protection mechanism of A1M should be based on the redox activity of the free thiolyl group of the C34 side-chain and a regulatory role of the K92, K118 and K130 residues.

INTRODUCTION

The Lipocalins are a protein family with approximately 50 members from bacteria, plants and animals [1-3]. The lipocalin proteins have similar structures but different, mostly non-related functions. They share a common fold, a β-barrel consisting of eight antiparallel β-strands with a closed bottom and an open end [4].

One member of the Lipocalin family, α_1-microglobulin (A1M), is a 26 kDa glycoprotein found in blood-plasma and interstitial fluid of all human tissues [5-7]. A1M is mainly synthesized in the liver, and expressed together with bikunin, a proteinase inhibitor and component of extracellular matrix [8]. The *AMBP*-gene codes for an A1M-bikunin precursor protein which is expressed, processed and cleaved before secretion of the two mature proteins separately into the blood-stream [9,10].

A1M has been shown to have reductase activity [11,12] as well as heme- and radical-binding properties [11,12] and it was suggested that the physiological function of A1M is to protect cells and tissues against oxidative stress induced by extracellular hemoglobin and other sources of free radicals and oxidants [6,13]. This is supported by several recent papers demonstrating that A1M protects cell cultures and organ explants against oxidative damage [3,14-16]. For example, A1M suppressed the cell death, apoptosis, and up-regulation of stress-response genes in the bystander cells of irradiated cell cultures, *i.e.* cells in the culture that were not directly exposed to the alpha-particles, but suffered indirect damage [17]. The bystander effect is induced by a propagation of stress factors from the directly targeted cells and manifests as cell death, genomic instability and changes in gene expression in the non-irradiated bystander cells surrounding the targeted cells [18-20]. Oxidants and ROS have been

Field Code Changed

suggested as mediators of the bystander effects [21-23]. It was also shown that A1M inhibited destruction of cells and extracellular matrix collagen in skin explants and keratinocyte cultures exposed to heme- and iron-induced oxidative stress [15].

We have previously reported that the free thiol group of cysteine 34 (C34) is critically involved in the reductase and radical scavenging activity of A1M [11,12]. According to a model of the three-dimensional structure of A1M [24], as well as the recently reported crystal structure[25], C34 is localized on a loop at the rim of the lipocalin pocket (Figure 1B). Three lysyl groups, K92, 118, and 130, localized on the inside of the upper part of the lipocalin pocket, were also shown to be crucial for the reductase activity [11].

We hypothesized that the reductase activity of A1M is important for its protective effects. To test this, we prepared and investigated wild type (wt)-A1M and three mutated forms of A1M: C(34)S-A1M, carrying a Cys→Ser substitution in position 34; K(3)T-A1M, with Lys→Thr substitutions in positions 92, 118 and 130; and a C(34)S/K(3)T-A1M mutant containing both types of mutations (Figure 1A) [26]. The reductase activities of these forms of A1M, as well as their ability to inhibit bystander effects in irradiated cell cultures and protect collagen fibers from oxidation, were investigated.

RESULTS

Preparation of recombinant A1M variants

The A1M variants were investigated by SDS-PAGE, MS analysis and thiol group reactivity (Figure 2). The same variants have previously been analyzed by RIA, fluorescence spectroscopy and far-UV circular dichroism [26]. All variants appeared pure, as determined by SDS-PAGE (Figure 2A). Consistent with the theoretical molecular masses, the K(3)T-A1M (22.56 kDa) and C(34)S/K(3)T-A1M (22.54 kDa) appeared somewhat smaller than the wt-A1M (22.64 kDa) and C(34)S-A1M (22.66). In the figure, all A1M-variants, except C(34)S/K(3)T-A1M, appear as a double-band and both bands of wt-A1M were identified as A1M by trypsin digestion and Maldi-MS/MS peptide sequencing, and contained the intact C-terminal tryptic peptide. The lower band is probably a result of a proteolytic cleavage at the N-terminus, since the N-terminal tryptic peptide was identified in the upper band but not in the lower band. All mutations were verified by MS/MS sequencing. The preparations shown in Figure 2A are representative for all the following experiments. We analyzed thiol groups in all the mutants using a quantitation kit (Figure 2B). As expected the C(34)S-A1M and the C(34)S/K(3)T-A1M mutants showed values close to zero, whereas wt- and K(3)T-A1M displayed similar amounts. However, less than one thiol group/mol A1M was found in both A1M-forms even after reduction with DTT. This suggests that the C34 sulfhydryl group is partially oxidized in both wt-A1M and K(3)T-A1M.

Field Code Changed

Protection of irradiated HepG2 cell cultures from irradiation-induced cell death by A1M mutants

We have previously shown that A1M counteracts the irradiation-induced cell death of both directly irradiated HepG2 cells and bystander cells, *i.e.* cells in the culture that were not

directly exposed to the alpha-particles, but suffered indirect damage . In order to clarify the mechanism by which A1M protects bystander cells we investigated whether the mutated forms of A1M could counteract the irradiation-induced cell death. HepG2 cells were irradiated with alpha-particles (1.8 Gy) and subsequently cultured in medium with or without 2 μM A1M. A significant decrease of cell death, measured as LDH leakage to the cell medium, after irradiation was observed when wt-A1M and K(3)T-A1M mutant were added whereas no decrease, or only a slight decrease, was seen in the presence of C(34)S-A1M or C(34)S/K(3)T-A1M (Figure 3A).

Inhibition of stress- and antioxidation gene response of irradiated HepG2 cell cultures by A1M variants

The levels of mRNA coding for the cell cycle regulatory genes p21 and p53 were analyzed by real time PCR (Fig 3B). Both genes were up-regulated by the irradiation, and the up-regulation was significantly reversed by the addition of wt-A1M. The same result was obtained with K(3)T-A1M, whereas the C(34)S and the C(34)/K(3)T mutants failed to reduce the irradiation-induced up-regulation of neither p21- or p53-genes. We also analyzed the expression of the antioxidation genes HO-1, GPX1 and A1M (Figure 3B). All three genes were strongly up-regulated by the irradiation, supporting the idea of oxidative stress as mediators of the bystander effect. The addition of wt-A1M significantly inhibited the irradiation-induced up-regulation of the A1M and GPX1-genes down to or below non-irradiated cells and to some extent the HO-1-gene. Both the wt-A1M and the K(3)T-A1M mutants were able to inhibit the up-regulation of the A1M- and GPX1-genes, and to some extent the HO-1-gene. This, was not the case when C(34)S-A1M or C(34)S/K(3)T-A1M were added, *i.e.* both failed to reduce the irradiation-induced up-regulation of A1M, HO-1 and GPX1.

Cell uptake of A1M-variants in irradiated HepG2 cell cultures

We have previously shown that the cellular uptake of A1M increases in irradiated cell cultures compared to non-irradiated control cultures [17]. To investigate the difference in uptake between the A1M variants, we measured the concentrations of A1M in both cells and medium, respectively, following irradiation (Figure 4). The cellular uptake of wt-A1M, C(34)S-A1M, K(3)T-A1M, and C(34)S/K(3)T-A1M was 0.8 %, 0.6 %, 0.7 % and 0.3 %, respectively, of total A1M in cells and medium.

Reductase activity of A1M-variants.

It was shown previously that A1M can reduce the ABTS-radical [12]. Therefore, we analyzed the capacity of the various forms of A1M to reduce the ABTS-radical, an optically stable free radical which is widely used for studies of antioxidant mechanisms and radical reactions [27], using the protein AGP [28] as negative control (Figure 5). Only wt-A1M reduced the ABTS radical whereas all the mutated forms displayed background activity, at the level of the non-reducing control protein AGP [11] which did not differ significantly from the mutated forms of A1M

Reduction of carbonyl groups on oxidized collagen by A1M-variants.

It was previously shown that A1M can remove pre-formed carbonyl groups on heme- and H_2O_2-oxidized collagen. This indicates a repair effect of the protein which also may be an effect of its reductase activity. [15]. Hence, we compared this activity of mutated A1M-variants. Collagen coated to microtiter plates was oxidized with 30 μM heme (Figure 6A) or 1 mM H_2O_2 (Figure 6B). Both heme and H_2O_2 generated a statistically significant increase in carbonyl groups. Wt-A1M was able to reduce the oxidation of collagen down to below the level of non-oxidized collagen, and the K(3)T-A1M mutant down to the level of non-oxidized

collagen. When oxidized with heme C(34)S-A1M showed only a slight reduction. When oxidized with H_2O_2 the C(34)S-A1M showed no reduction capacity. No changes in reduction capacity of any of the variants were seen at longer times than 15 min (not shown).

DISCUSSION

The main message of the present report is that the protective effect of A1M in irradiated cell cultures and the reduction of oxidized collagen are strongly dependent on the cysteine residue in position 34.

To ascertain that differences in functions of the various forms of A1M are due to the amino acid substitutions rather than impurities or effects of incorrect folding, we investigated biochemical properties of the recombinant A1M-species. The proteins appeared highly purified on SDS-PAGE-gels (Figure 2A). The wt-, C(34)S- and K(3)T-A1M-variants were seen as a double band where the minor band migrated with a slightly lower apparent molecular mass than the major band. Both bands were shown to consist of A1M, using mass spectrometry/tryptic peptide mapping. The intact C-terminal tryptic peptide was found in both bands, suggesting that the difference in migration is due to proteolytic cleavage of the N-terminus which contains a His_8-tag. This is also supported by the peptide mapping since the full-length N-terminal tryptic peptide was detected in the upper band but not the lower. The small size difference (<1 kDa) and the fact that both bands were eluted from a Ni-agarose-column during the purification, suggesti that some of the His-residues remained on the peptide. It was shown previously, however, that the His-tag does not contribute to, or interfere with, the reductase activities or the cell protection effects of A1M [11,12,14], and we therefore expect that the two bands of each A1M-variant have similar reductase and protection effects in this investigation.

Field Code Changed
Field Code Changed
Field Code Changed

The surface epitopes on the A1M variants were previously analyzed by radioimmunoassay using antibodies against A1M from human urine [26]. The ability of the recombinant A1M-

Field Code Changed

variants to inhibit the binding of the polyclonal antibodies to human urine A1M was very similar, suggesting that the mutated A1M-variants have a similar three-dimensional conformation as wt-A1M. This could be confirmed by fluorescence spectroscopy and circular dichroism [26]. We therefore conclude that the different effects of the A1M-variants seen in this study are due to amino acid substitutions *per se* and not a result of folding differences induced by the mutations.

Field Code Changed

It was recently reported that the irradiation-induced damage of both directly targeted cells and bystander cells was inhibited by A1M. We hypothesized that the four side-chains C34, K92, K118 and K130 are involved in the protection mechanism because they have been shown to have an impact on the reductase activity of A1M [11] and studied this using site-directed mutagenesis. An increase in cell death (LDH leakage), up-regulation of the cell cycle regulatory genes p21 and p53 and up-regulation of the antioxidation genes HO-1, GPX1 and A1M were seen in the irradiated cell cultures, and all these responses were significantly inhibited by wt-A1M, supporting and extending previous findings. In contrast, no inhibition was seen by the C(34)S-A1M mutant and the C(34)S/K(3)T-A1M mutant, suggesting that the C34 side-chain is a major requirement for the protective effects of A1M against irradiation-induced cell death and cell damage. The K(3)T-A1M mutant, on the other hand, significantly inhibited cell death and up-regulation of all five genes, although not to the same extent as wt-A1M. Taken together, the results suggest that the C34 side-chain is of major importance to the protection mechanism of A1M and that the K92, K118 and K130 side-chains seem to have some impact on the protection activity of A1M.

Field Code Changed

Two possible mechanistic explanations of the protection effects of A1M were studied in this investigation: cellular uptake and reductase activity. It was previously shown that uptake of

A1M to the cells increases in irradiated cells [17]. Here, it was shown that the cellular uptake of wt-A1M was higher than the other variants of A1M (Figure 4). Significantly less of C(34)S-A1M and C(34)S/K(3)T-A1M were taken up by the cells, while the K(3)T-A1M differed only slightly from the wt-A1M, indicating that the C34 side-chain is involved in the cell-uptake mechanism. Previous studies suggest the presence of a cell-surface receptor [29,30] as well as intracellular A1M-binding proteins [14,17] and it can be speculated that the C34 side-chain is involved in the recognition by these receptors either as part of a protein-protein interaction or as a result of its participation in the redox activities of A1M. Thus, the cell uptake parallels the protective effects and the lower uptake of the C34-thiol group-lacking A1M-variants may therefore partly explain their lack of protection against irradiation damage. The cell volume in our experimental setup was less than 1% of the volume of the medium (not shown), suggesting that the concentration of wt-A1M, after uptake, was roughly the same, or higher, inside the cells as in the medium, i.e. >2 uM. This relatively high concentration may explain the rather efficient protection of the cells from irradiation damage.

The reductase activity of A1M was studied using two different substrates, the ABTS-radical and oxidized collagen, both of which have previously been shown to be reduced by A1M [12,15]. Only wt-A1M reduced the ABTS-radical whereas all the mutated forms displayed background activity, at the same level as the non-reducing control protein AGP (Figure 5). A somewhat different result was obtained with oxidized collagen, which was reduced by both wt- and K(3)T-A1M and to a lesser extent by C(34)S-A1M . This suggests that the C34 side-chain is crucial for the reductase activity towards both substrates, and that the lysyl side-chains are important for the reduction of the ABTS-radical and play a minor role in the reduction of oxidized collagen. This is in agreement with previous reports that the C34 residue is of central importance for the reductase activity [11,12]. The three lysyl residues

Field Code Changed
Field Code Changed
Field Code Changed
Field Code Changed
Field Code Changed
Field Code Changed
Field Code Changed
Field Code Changed

were shown to influence the reduction of other substrates [11] but have not previously been studied with ABTS-radical or oxidized collagen. It is thus likely that K92, K118 and K130 are involved in the reductase activities of A1M to different extents depending on substrate identity, kinetics and stoichiometry.

Two different roles of the K92, K118 and K130 side-chains have been proposed previously. First, it was suggested that they may create a positive electrostatic environment around the C34 side-chain (1), since the crystal structure and three-dimensional model of A1M show that they are localized closely together around the opening of the lipocalin pocket[25]. This would lower the pK_a of the thiol group, promote de-protonation, and hence favor its oxidation. Secondly, as described above, these side-chains are modified in urinary and amniotic A1M [31,32] and they have therefore been proposed to function as acceptors of covalently trapped free radicals, together with several other side-chains of the protein [12]. Thus, both these roles of K92, 118 and 130, *i.e.* enhancement of the redox activity of C34 and as sites of radical trapping, may explain the partial impact of these residues in the cell protection, and reduction of oxidized collagen and ABTS-radicals.

It was reported that the reaction with the ABTS-radical results in covalent adduction of a half ABTS-molecule to the Y22 and Y132 side-chains of A1M [12]. This indicates the Y22 and Y132 side-chains as acceptors of covalently trapped radicals, by analogy to K92, 118 and 130. Interestingly, the side-chain of Y132 is only accessible from the inside of the lipocalin pocket approximately two-thirds down towards the bottom [25]. This, and the location of the three lysyl residues higher up in the pocket, suggests that the ABTS-radical can be transiently complex-bound in the lipocalin pocket, and a possible role for the pocket in the radical scavenging mechanism of A1M.

Field Code Changed
Field Code Changed
Field Code Changed
Field Code Changed
Field Code Changed
Field Code Changed
Field Code Changed

A unifying model of the protection mechanism of A1M is that the molecule acts as a "radical sink". According to this model, which was proposed in detail previously [12], each A1M-molecule can eliminate at least 8-9 radicals by a semi-catalytic covalent trapping mechanism that can be summarized as a series of subsequent reactions: 1) A one-electron reduction of a substrate (for example an ABTS-radical) by the C34 thiolate group, yielding a thiolyl radical; 2) an intramolecular electron-transfer between any of the K92, K118, K130, Y22 or Y132 side chains and the oxidized C34 thiolyl which re-generates the thiol for another reduction reaction and creates an oxidized tyrosyl or lysyl radical; 3) a covalent adduction reaction between the tyrosyl/lysyl radical and a radical substrate (for example an ABTS-radical). The reaction cycle can then be repeated with remaining lysyl/tyrosyl side-chains. This hypothetical reaction scheme thus results in covalent binding of *n* ABTS-radicals plus reduction of (*n*+1) ABTS-radicals, where *n*=5 when the five side-chains K92, K118, K130, Y22 and Y132 are involved in reaction 3. Applied to the ABTS-radical, the total number of eliminated radicals per A1M-molecule was experimentally determined to nine, and the number of reduced radicals was five [12]. Hence, this suggests that *n*=4 in the reaction with the ABTS-radical, *i.e.* four ABTS-radicals are covalently bound to lysyl/tyrosyl side-chains. It can be concluded that such a semi-catalytic mechanism gives A1M an approximately 10-fold higher radical-clearing capacity than other physiological molecules carrying a free thiol group, *e.g.* albumin and glutathione. Likewise, Trolox, a water soluble analog of vitamin E which is considered as a highly efficient low-molecular weight radical scavenging antioxidant, was shown to have a 1:1 stoichiometry of reduction towards ABTS, a 10-fold lower capacity than A1M [12]. *In vivo*, the stoichiometry of reduction and covalent trapping reactions may differ for various radical substrates since the size, charge and shape determine the availability for covalent adduction to A1M side-chains. Eventually, the side-chains of the

Field Code Changed

Field Code Changed

Field Code Changed

A1M-molecule becomes saturated and the protein is cleared from the tissues by the blood and subsequent glomerular filtration in the kidneys.

We have shown in this work that the antioxidative protection of cells and collagen by A1M is totally dependent on the free thiolyl group of the C34 side-chain and regulated by the K92, K118 and K130 residues. Knowledge of the protective mechanism of A1M is important for potential future therapeutic applications in diseases with oxidative stress.

MATERIALS AND METHODS

Reagents and proteins

Hydrogen peroxide was bought from Acros Organics, NJ, U.S.A. and DNP (dinitrophenyl-hydrazine) from Sigma. Swine anti-rabbit IgG-horseradish peroxidase (HRP) was purchased from Dako A/S (Glostrup, Denmark). Chicken anti-human A1M antibodies were prepared at Agrisera AB, Vännäs, Sweden by immunization with human urine A1M, purified at our laboratory, and subsequent purification of the IgY-fraction. Rabbit anti-chicken/turkey IgG-HRP was from Invitrogen (Camarillo, CA, U.S.A.). 3´,3´,5,5;-Tetra Methyl Benzidine Single Solution (TMB) was from Invitrogen (Frederic, MD, U.S.A.). α_1-acid glycoprotein (AGP) and 2,2´-Azino-bis(3-ethyl-benzo-thiazoline-6-sulphonic acid) diammonium salt (ABTS) and DL-Dithiothreitol (DTT) were from Sigma. Heme (hemin; ferriprotoporphyrin IX chloride) was purchased from Porphyrin Products, Inc. (Logan, UT, U.S.A.). Stock solutions of heme were prepared by dissolving heme in DMSO to 10 mM and used within 10 h. Thiol and Sulfide Quantitation Kit was from Molecular Probes (Leiden, Netherlands).

Recombinant A1M

Wild-type (Wt) and mutated variants of A1M were expressed in *Escherichia coli* (*E. coli*). Using site-directed mutagenesis a Cys → Ser substitution was introduced at amino acid position 34 in the C(34)S-A1M mutant, and Lys → Thr substitutions at positions 92, 118, and 130 in the K(3)T-A1M mutant. The four forms of recombinant A1M illustrated in Figure 1A, Wt-A1M, C(34)S-A1M, K(3)T-A1M and C(34)S/K(3)T-A1M, were purified and refolded as described [26].

Field Code Changed

Cell culture

The human hepatoma cell line HepG2 was obtained from the American Type Culture Collection (Rockville, MD) and cultured in RPMI 1640 with GlutaMAX^{TM}I medium containing 10 % fetal bovine serum (FBS), 100 μg/ml antibiotics (penicillin and streptomycin) and 100 μg/ml antimycotics (amphotericin B). The cells were incubated at 37ºC in an atmosphere of 5 % CO_2 and trypsinated as described [33]. When experiments were carried out the HepG2 cells were at a confluence rate of approximately 80-90 %.

Field Code Changed

Irradiation procedure

The irradiations were performed using alpha particles (helium ions) from a ^{241}Am source as described previously [17] , collimating the beam using a Mylar mask. Approximately of 0.02% (1.13 mm^2 of totally 5671 mm^2) of the total number of cells in the petri dish were hit by irradiation and 99.98 % of the cells were bystander cells, *i.e.* not exposed to irradiation. The measured dose rate from the source through the hole in the mask was 0.067 Gy/s. The cells received an absorbed dose of 1.8 Gy, *i.e.* the irradiation time was 27 seconds.

Field Code Changed

LDH analysis

The concentration of LDH in the cell culture media was used to estimate the degree of cytolysis induced by irradiation, and was measured using CytoTox96® Non-Radioactive Cytotoxicity Assay Kit from Promega (Madison, WI, U.S.A.). The analysis was performed according to the instructions from the manufacturer.

Radio-immunoassay (RIA)

Radiolabelling of A1M with ^{125}I was done using the chloramine T method [34]. Protein-bound iodine was separated from free iodide by gel-chromatography on a Sephadex G-25

Field Code Changed

column (PD10, Amersham Biotech). A specific activity of around 0.1 – 0.2 MBq/µg protein was obtained. RIA was performed as described [35]. The ^{125}I activity of the pellets was measured in a Wallac Wizard 1470 gamma counter (Perkin Elmer Life Sciences). To determine uptake of A1M, the cells were washed thoroughly with PBS to exclude any non-bound A1M and lyzed by resuspension in 50mM Tris-HCl pH 8,0; 2mM EDTA; 1% NP40; 1µg/µl pepstatin; 5µg/µl antipain; 10µg/µl leupeptin. The suspension was centrifuged for 10 min at 4°C and 10,000xg, and the supernatant diluted in the assay buffer [35].

Field Code Changed

Field Code Changed

SDS-PAGE

Sodium dodecyl sulfate-polyacrylamide gel electrophoresis (SDS-PAGE) was performed as described by Laemmli [36]. The gel was run under reducing conditions by mixing the samples with sample buffer containing 2 % (v/v) mercaptoethanol and then boiling for 1 minute. The gels were stained with Coomassie Brilliant Blue R-250 (BDH Chemicals, Ltd. Poole, UK).

Field Code Changed

Protein identification by MS peptide mapping and sequencing analysis.

The protein analysis was performed by Alphalyse A/S (Odense, Denmark). Briefly, the protein samples were reduced and carbamidomethylated, and subsequently digested with trypsin. The resulting peptides were concentrated on a ZipTip micropurification column and eluted onto an anchorchip target for analysis on a Burker Autoflex Speed MALDI TOF/TOF instrument. MALDI MS/MS was performed on 15 peptides for partial sequencing. The MS and MS/MS spectra were combined and used for database searching. The data were searched against in-house protein databases downloaded from NBCI, including the NRDB database.

Determination of protein carbonyl groups

Collagen type I Chrono-Par nr. 385 was from (Chrono-Log, Havertown, PA U.S.A.) was coated at 5µg/ml on a 96-well microtiter plate (Nunc Maxitorp, WVR International, Sweden) overnight at 4°C. Oxidation of collagen was done by adding heme or hydrogen peroxide as indicated in the Figure legends. After washing, A1M was incubated for various time-periods (15 min-2h) with the oxidized collagen as described for each experiment in the Figure legends. The plate was washed and carbonyl groups determined by DNP-hydrazine conjugation and incubation with anti-DNP antibodies (Invitrogen, Eugene, OR, U.S.A) according to the method of Buss et al [37] as detailed [15].

Field Code Changed

Field Code Changed

RNA isolation and real-time PCR

Total RNA was isolated from HepG2 cells and cDNA prepared by reverse transcription as described . Real-time PCR was then used to quantify the p21, p53, A1M , heme oxygenase 1 (HO-1), and glutathione peroxidase 1 (GPX1) mRNA. Human glyceraldehyde-3-phosphate dehydrogenase (G3DPH) was used to normalize the amounts of mRNA, and the relative amounts are depicted in the figure as ΔΔCt. Primers were designed as described with the addition of, GPX1 forward primer 5´-CCAGTCGGTGTATGCCTTCT-3´, reverse primer 5´-TGCAGCTCGTTCATCTGG-3´. The expression was analyzed using MaximaTM SYBR Green/Fluorescein qPCR Master Mix (Fermentas). Amplification was performed at 55ºC for 40 cycles in iCycler Thermal Cycler (BioRad, Hercules, CA, U.S.A.) and data analyzed using iCycler iQ Optical System Software.

Reduction of ABTS radical

The reductase activity of A1M was analyzed by reaction with ABTS-radical as previously described [12]. Briefly, a stock solution of ABTS-radical was prepared by oxidation of 7 mM

Field Code Changed

ABTS solution with 2.45 mM potassium persulfate allowing the solution to react for at least 6 h. The solution was kept in the dark at RT and used within 24 h. Four µM A1M and control protein were added to a 56 µM ABTS-radical solution in 25 mM sodium phosphate, pH 8.0. The absorbance was read every 5 s at 735 nm for 1 min.

Thiol and sulfide determination

The thiol quantitation of A1M was determined using Thiol and Sulfide Quantitation assay Kit. The measurements were performed according to the instructions from the manufacturer. The method is based on a disulfide inhibition by a papain derivative. The activation of the enzyme is measured using chromogenic papain substrate. L-cystein is used as a standard the accurate concentration of which is determined with Ellman´s reagent. Before thiol quantitation 100 µg of Wt and K(3)T A1M were incubated with 10 mM DTT for 1 h followed by dialysis in 5 L 20 mM Tris-HCl; pH 8.0 for 3 h.

Statistical analysis

One-way ANOVA with Tukey post-hoc test was performed using GraphPad Prism version 5.0c for Windows, GraphPad Software, La Jolla California USA, www.graphpad.com. Significance level: $P< 0.05$.

ACKNOWLEDGEMENTS

This work was supported by the Swedish Research Council [project no. 7144], governmental ALF research grants to Lund University and Lund University Hospital, the Royal Physiographic Society in Lund, the Foundations of Greta and Johan Kock, Alfred Österlund, the Blood and Defence Network, Lund University, the Crafoord Foundation (20081029), CELLION (MRTN-CT-2003-503923), and A1M Pharma AB.

COMPETING INTERESTS

The authors MG and BÅ are part-founders and hold shares in the company A1M Pharma AB. This does not alter the authors' adherence to all the Free Radical Research policies on sharing data and materials.

LIST OF ABBREVATIONS

A1M	α_1-microglobulin
ABTS	2,2´-Azino-bis(3-ethyl-benzo-thiazoline-6-sulphonic acid) diammonium salt
AGP	α_1-acid glycoprotein
AMBP	A1M-bikunin precursor protein
BSA	Bovine serum albumin
DNP	2,4-dinitrophenylhyrazine
DTT	DL-Dithiothreitol
FBS	Fetal bovine serum
GPX1	glutathione peroxidase 1
HepG2	Human hepatoma cell line
HO-1	Heme oxygenase-1
HRP	Horseradish peroxidase
LDH	Lactate dehydrogenase
ROS	Reactive oxygen species
TMB	3´,3´,5,5;-Tetra Methyl Benzidine

REFERENCES

[1] Flower DR. The lipocalin protein family: structure and function. Biochem J 1996;318 (Pt 1):1-14.

[2] Åkerström B, Flower DR, Salier JP. Lipocalins: unity in diversity. Biochim Biophys Acta 2000;1482(1-2):1-8.

[3] Åkerström B, Borregaard N, Flower DR, Salier JP, editors. Lipocalins: An introduction. Georgetown, Texas: Landers Bioscience; 2006.

[4] Ganfornina MD, Sanchez D, Greene LH, Flower DR, editors. The lipocalin protein family: Protein sequence, structure and relationship to the calycin superfamily. Georgetown, Texas: Landers Bioscience; 2006.

[5] Ekström B, Berggård I. Human α_1 -microglobulin . Purification procedure, chemical and physiochemical properties. J Biol Chem 1977;252(22):8048-57.

[6] Åkerström B, Lögdberg L, editors. α_1 -microglobulin. Georgetown, Texas: Landers Bioscience; 2006.

[7] Åkerström B, Lögdberg L. An intriguing member of the lipocalin protein family: α_1 -microglobulin. Trends Biochem Sci 1990;15:240-243.

[8] Kaumeyer JF, Polazzi JO, Kotick MP. The mRNA for a proteinase inhibitor related to the HI-30 domain of inter-alpha-trypsin inhibitor also encodes α_1 -microglobulin (protein HC). Nucleic Acids Res 1986;14(20):7839-50.

[9] Lindqvist A, Bratt T, Altieri M, Kastern W, Åkerström B. Rat α_1 -microglobulin: co-expression in liver with the light chain of inter-alpha-trypsin inhibitor. Biochim Biophys Acta 1992;1130(1):63-7.

[10] Bratt T, Olsson H, Sjöberg EM, Jergil B, Åkerström B. Cleavage of the α_1 -microglobulin - bikunin precursor is localized to the Golgi apparatus of rat liver cells. Biochim Biophys Acta 1993;1157(2):147-54.

[11] Allhorn M, Klapyta A, Åkerström B. Redox properties of the lipocalin α_1 -microglobulin : reduction of cytochrome c, hemoglobin, and free iron. Free Radic Biol Med 2005;38(5):557-67.

[12] Åkerström B, Maghzal GJ, Winterbourn CC, Kettle AJ. The lipocalin α_1 -microglobulin has radical scavenging activity. J Biol Chem 2007;282(43):31493-503.

[13] Olsson MG, Allhorn M, Bulow L, Hansson SR, Ley D, Olsson ML, Schmidtchen A, Akerstrom B. Pathological Conditions Involving Extracellular Hemoglobin: Molecular Mechanisms, Clinical Significance, and Novel Therapeutic Opportunities for alpha(1)-Microglobulin. Antioxid Redox Signal 2012;Epub ahead of print.

[14] Olsson MG, Olofsson T, Tapper H, Åkerström B. The lipocalin α_1 -microglobulin protects erythroid K562 cells against oxidative damage induced by heme and reactive oxygen species. Free Radic Res 2008;42(8):725-36.

[15] Olsson MG, Allhorn M, Larsson J, Cederlund M, Lundqvist K, Schmidtchen A, Sörensen OE, Mörgelin M, Åkerström B. Up-Regulation of A1M/α_1 -microglobulin in Skin by Heme and Reactive Oxygen Species Gives Protection from Oxidative Damage. PLoS One 2011;6(11):e27505.

[16] May K, Rosenlöf L, Olsson MG, Centlow M, Mörgelin M, Larsson I, Cederlund M, Rutardottir S, Siegmund W, Schneider H and others. Perfusion of human placenta with hemoglobin introduces preeclampsia-like injuries that are prevented by α_1 -microglobulin Placenta 2011;32(4):323-32.

[17] Olsson MG, Nilsson EJ, Rutardottir S, Paczesny J, Pallon J, Akerstrom B. Bystander cell death and stress response is inhibited by the radical scavenger alpha(1)-microglobulin in irradiated cell cultures. Radiat Res 2010;174(5):590-600.

[18] Little JB, Azzam EI, de Toledo SM, Nagasawa H. Bystander effects: intercellular transmission of radiation damage signals. Radiat Prot Dosimetry 2002;99(1-4):159-62.
[19] Mothersill C, Seymour C. Radiation-induced bystander effects: past history and future directions. Radiat Res 2001;155(6):759-67.
[20] Prise KM, Folkard M, Michael BD. A review of the bystander effect and its implications for low-dose exposure. Radiat Prot Dosimetry 2003;104(4):347-55.
[21] Azzam EI, de Toledo SM, Little JB. Oxidative metabolism, gap junctions and the ionizing radiation-induced bystander effect. Oncogene 2003;22(45):7050-7.
[22] Lyng FM, Seymour CB, Mothersill C. Production of a signal by irradiated cells which leads to a response in unirradiated cells characteristic of initiation of apoptosis. Br J Cancer 2000;83(9):1223-30.
[23] Lyng FM, Seymour CB, Mothersill C. Initiation of apoptosis in cells exposed to medium from the progeny of irradiated cells: a possible mechanism for bystander-induced genomic instability? Radiat Res 2002;157(4):365-70.
[24] Villoutreix BO, Åkerström B, Lindqvist A. Structural model of human α_1 -microglobulin : proposed scheme for the interaction with the Gla domain of anticoagulant protein C. Blood Coagul Fibrinolysis 2000;11(3):261-75.
[25] Meining W, Skerra A. The crystal structure of human alpha(1)-microglobulin reveals a potential haem-binding site. Biochem J 2012;445(2):175-82.
[26] Kwasek A, Osmark P, Allhorn M, Lindqvist A, Åkerström B, Wasylewski Z. Production of recombinant human α_1 -microglobulin and mutant forms involved in chromophore formation. Protein Expr Purif 2007;53(1):145-52.
[27] Miller NJ, Rice-Evans CA. Factors influencing the antioxidant activity determined by the ABTS.+ radical cation assay. Free Radic Res 1997;26(3):195-9.
[28] Fournier T, Medjoubi NN, Porquet D. Alpha-1-acid glycoprotein. Biochim Biophys Acta 2000;1482(1-2):157-71.
[29] Fernandez-Luna JL, Leyva-Cobian F, Mollinedo F. Identification of the protein HC receptor. FEBS Lett 1988;236(2):471-4.
[30] Wester L, Michaelsson E, Holmdahl R, Olofsson T, Akerstrom B. Receptor for alpha1-microglobulin on T lymphocytes: inhibition of antigen-induced interleukin-2 production. Scand J Immunol 1998;48(1):1-7.
[31] Sala A, Campagnoli M, Perani E, Romano A, Labo S, Monzani E, Minchiotti L, Galliano M. Human α_1 -microglobulin is covalently bound to kynurenine-derived chromophores. J Biol Chem 2004;279(49):51033-41.
[32] Berggård T, Cohen A, Persson P, Lindqvist A, Cedervall T, Silow M, Thogersen IB, Jönsson JA, Enghild JJ, Åkerström B. α_1 -microglobulin chromophores are located to three lysine residues semiburied in the lipocalin pocket and associated with a novel lipophilic compound. Protein Sci 1999;8(12):2611-20.
[33] Åkerström B, Bratt T, Enghild JJ. Formation of the alpha α_1 -microglobulin chromophore in mammalian and insect cells: a novel post-translational mechanism? FEBS Lett 1995;362(1):50-4.
[34] Greenwood FC, Hunter WM, Glover JS. The Preparation of I-131-Labelled Human Growth Hormone of High Specific Radioactivity. Biochem J 1963;89:114-23.
[35] Plesner T, Norgaard-Pedersen B, Boenisch T. Radioimmunoassay of β2-microglobulin. Scand J Clin Lab Invest 1975;35(8):729-35.
[36] Laemmli UK. Cleavage of structural proteins during the assembly of the head of bacteriophage T4. Nature 1970;227(5259):680-5.
[37] Buss H, Chan TP, Sluis KB, Domigan NM, Winterbourn CC. Protein carbonyl measurement by a sensitive ELISA method. Free Radic Biol Med 1997;23(3):361-6.
[38] Takagi T, Takagi K, Kawai T. Complete amino acid sequence of human α_1 -microglobulin. Biochem Biophys Res Commun 1981;98(4):997-1001.

[39] Amoresano A, Minchiotti L, Cosulich ME, Campagnoli M, Pucci P, Andolfo A, Gianazza E, Galliano M. Structural characterization of the oligosaccharide chains of human α_1 -microglobulin from urine and amniotic fluid. Eur J Biochem 2000;267(7):2105-12.

[40] Newcomer ME, Ong DE. Purification and crystallization of a retinoic acid-binding protein from rat epididymis. Identity with the major androgen-dependent epididymal proteins. J Biol Chem 1990;265(22):12876-9.

LEGENDS TO FIGURES

FIGURE 1. **Schematic representation of A1M variants analyzed in this article.** (**A**) Human plasma and urine A1M contain three carbohydrate moieties at glycosylation sites T5, N17 and N96 [38,39]. Recombinant A1M was expressed in *E.coli*. as four variants: Wt A1M; a C(34)S mutant with a Cys → Ser substitution at position 34; a K(3)T mutant with Lys → Thr substitutions at positions 92, 118, and 130; and a C(34)S/K(3)T mutant with both of the above-mentioned mutations. All four recombinant variants have an N-terminal His_8-tag preceeding the natural N-terminus. Non-mutated amino acid positions are shown in regular font style and their mutated counterparts in bold face. (**B**) Three-dimensional structure of A1M. The illustration was generated using a Swiss-Pdb Viewer and Swiss Model (http://spdbv.vital-it.ch/) [40] using co-ordinates from the crystal structure of human A1M[25]. β-strands and α-helices are shown in grey. Side-chains of C34, K92, K118, K130 are shown by space-filling (black). N-terminal residues (1-7) and C-terminal residues (172-183) are not included. The model is viewed from the side of the β-barrel (top) and top view looking into the hydrophobic pocket (bottom).

Field Code Changed
Field Code Changed
Field Code Changed

FIGURE 2. **Size, purity, immunoreactivity and thiol activity of the four variants of recombinant A1M.** (**A**) SDS-PAGE was performed in the presence of mercaptoethanol (T= 12 %, C = 3.3). Approximately 5 µg of Wt (lane 1), C(34)S (lane 2), K(3)T (lane 3), and C(34)S/K(3)T (lane 4) were applied to the gel and stained with Coommassie Bands a) and b) marked with arrows analyzed by trypsin cleavage and MALDI-MS/MS analysis. (**B**) 7µg of the A1M variants was added to each well of a microtiter plate and 6 µl of a cystamine solution (0.1 mM). 100 µl of papain-$SSCH_3$ was the added and incubated for 1h at R.T. 100 µl of L-BAPNA solution (4.9 mM) was added to each well and incubated for 1h at R.T. Absorbance

was read at 405 nm. Previous to analysis, wt- and K(3)T-A1M were reduced by incubation with 10 mM DTT and dialysis. The values were plotted as mean of triplicates ± SD. Statistical comparison between groups was made using one-way ANOVA with Tukey post-hoc test. F(4, 10) = 7241; P< 0.0001. * P<0.05.

FIGURE 3. **Cell-protective and antioxidative properties of A1M-variants in irradiated HepG2 cells.** HepG2 cells were cultured to approximately 80-90 % confluence. Cells were irradiated with 1.8 Gy using alpha particles (helium ions) from a ^{241}Am source. Immediately after irradiation, fresh medium with 0 or 2 μM A1M was added and the cells cultured for 24 hours. (**A)** Medium was harvested and analysed for LDH leakage as described in Materials and Methods. The percentage (LDH measured in cell medium) of max (LDH measured in cell medium of irradiated cells) was plotted as mean of triplicates ± SD. In this figure, the effect of C(34)S/K(3)T-A1M on irradiated cells was studied in a separate experiment (dashed line), but normalized against control cells (0% LDH-release, Abs ^{490} = 0,66) and irradiated cells (100% LDH-release, Abs. ^{490} = 1,22). (**B**) Cells were harvested and mRNA levels of p21, p53, HO-1, A1M and GPX1 determined by real-time PCR as described in Materials and Methods. mRNA threshold cycles in non-irradiated cells or irradiated cells cultivated with added A1M were normalized against G3DPH and ΔΔCt was calculated by normalizing against non-irradiated cell cultures. In the figures, the effect of C(34)S/K(3)T-A1M on irradiated cells was studied in a separate experiment (dashed line). The inhibitions by the A1M-groups were compared to irradiated cultures using one-way ANOVA with Tukey post-hoc test. A1M, F(4, 20) = 13.44; P< 0.0001. HO-1, F(4, 18) = 1.218; P=0,34. P21, F(4, 25) =7.28; p=0.0005. p53, F(4, 25)= 28,89; p<0.0001. GPX1, F(4, 26) = 13.51; p<0.0001. LDH, F(4, 31) = 113,6; P<0,0001. * P<0.05.

FIGURE 4. **Uptake of A1M-variants in irradiated HepG2 cell cultures.** HepG2 cells were cultured to approximately 80-90 % confluence. Cells were irradiated with 1.8 Gy using alpha particles (helium ions) from a ^{241}Am source. Immediately after irradiation, fresh medium with 0 or 2 μM A1M was added and the cells incubated for 24 hours. Cells and medium were harvested and the protein concentration of A1M was determined by RIA. The percentage of A1M in the cell suspension of total A1M was plotted as mean of triplicates ± SD. Statistical comparison between the mutated A1M forms and Wt-A1M was made using one-way ANOVA with Tukey post-hoc test. , $F(3, 20) = 14{,}96$; $P < 0.0001$. * $P<0.05$.

FIGURE 5. **Reduction of ABTS-radical by A1M. (A)** ABTS-radical reduction activity was measured by adding the four recombinant A1M-variants or AGP to a final concentration of 4 μM, to a 56 μM ABTS-radical solution in 25 mM Na-phosphate, pH 8, reading the absorbance at 735 nm every 5 sec. Results from triplicate experiments are presented as mean ± SD. ●: Wt, Δ: C(34)S, ▲: K(3)T, □: C(34)S/K(3)T, ■: AGP. (**B**) The reaction rates (μM/s) of the reduction af ABTS radical by the various forms of A1M were calculated as the absolute values of the slopes of a line drawn by regression analysis of the points during the first 15 s, including time point zero. Results from triplicate experiments are presented as mean ± SD. Statistical comparison between the mutated A1M forms and Wt-A1M was made using one-way ANOVA with Tukey post-hoc test. , $F(4, 10) = 21{,}83$; $P < 0.0001$. No statistically significant difference was found between the mutated A1M forms and the control protein AGP. * $P<0.05$.

FIGURE 6. **Reduction of carbonyl groups on oxidized collagen by A1M.** Collagen was coated on microtiter plates overnight, washed and oxidized by incubation with 30 μM heme (**A**) or 1 mM H_2O_2 (**B**) for 2h. After washing, 0.3 μM A1M was added and incubated for 2 h.

Carbonyl groups were measured by ELISA as described [15,37]. In the figures, non-oxidized collagen was set as zero (Abs^{450} = 0.47 ^{H_2O_2}, 0.105 ^{Heme}) and the degree of reduction of the carbonyl groups is presented as percent of maximum (=oxidant only, Abs^{450} = 0.58 ^{H_2O_2}, 0.12 ^{Heme}). Results from triplicate experiments are presented as mean ± SD. Statistical comparison between collagen incubated with or without addition of A1M was made using One-way ANOVA with Tukey post-hoc test. H_2O_2 oxidized collagen, $F(4, 17) = 30{,}63$; $P < 0{,}0001$. Heme oxidized collagen, $F(4,14) = 18{,}3$; $P < 0{,}0001$. * $P<0.05$.

Field Code Changed

Field Code Changed

A

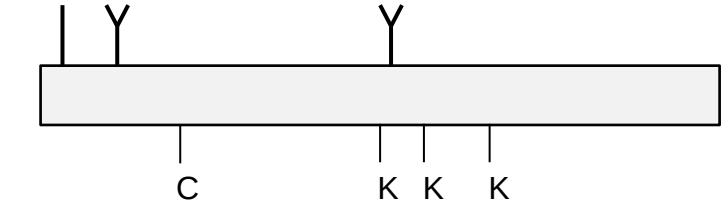

Plasma/
urine A1M

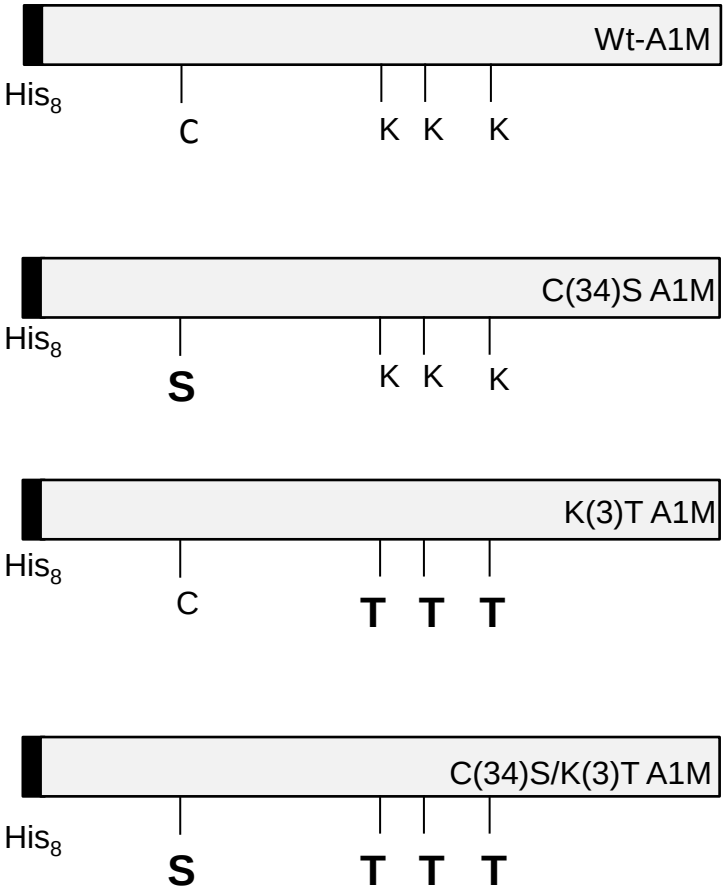

Recombinant A1M

B

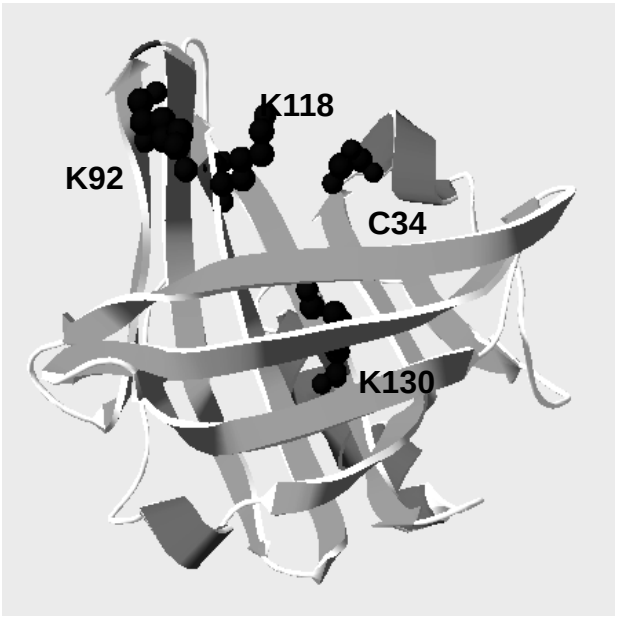

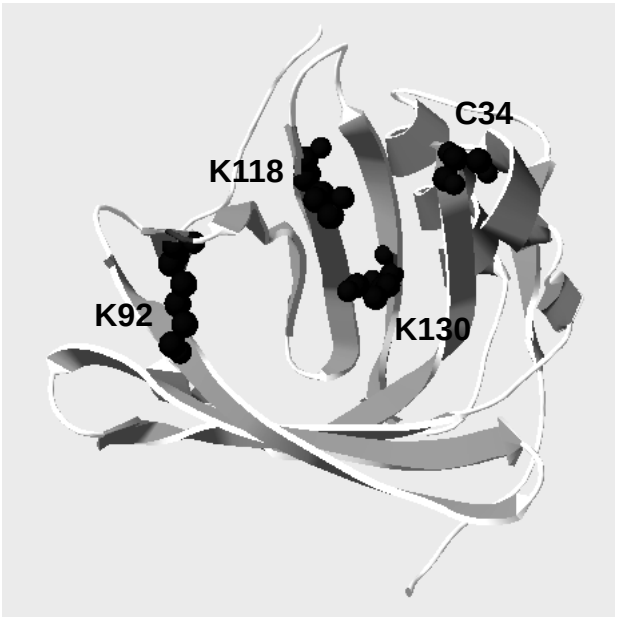

A

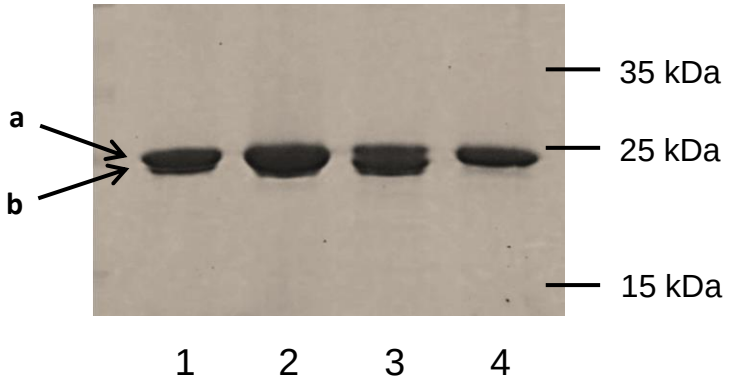

a)

```
  1 MHHHHHHHHD DDDKGPVPTP PDNIQVQENF NISRIYGKWY NLAIGSTCPW
 51 LKKIMDRMTV STLVLGEGAT EAEISMTSTR WRKGVCEETS GAYEKTDTDG
101 KFLYHKSKWN ITMESYVVHT NYDEYAIFLT KKFSRHHGPT ITAKLYGRAP
151 QLRETLLQDF RVVAQGVGIP EDSIFTMADR GECVPGEQEP EPILIPR
```

b)

```
  1 MHHHHHHHHD DDDKGPVPTP PDNIQVQENF NISRIYGKWY NLAIGSTCPW
 51 LKKIMDRMTV STLVLGEGAT EAEISMTSTR WRKGVCEETS GAYEKTDTDG
101 KFLYHKSKWN ITMESYVVHT NYDEYAIFLT KKFSRHHGPT ITAKLYGRAP
151 QLRETLLQDF RVVAQGVGIP EDSIFTMADR GECVPGEQEP EPILIPR
```

B

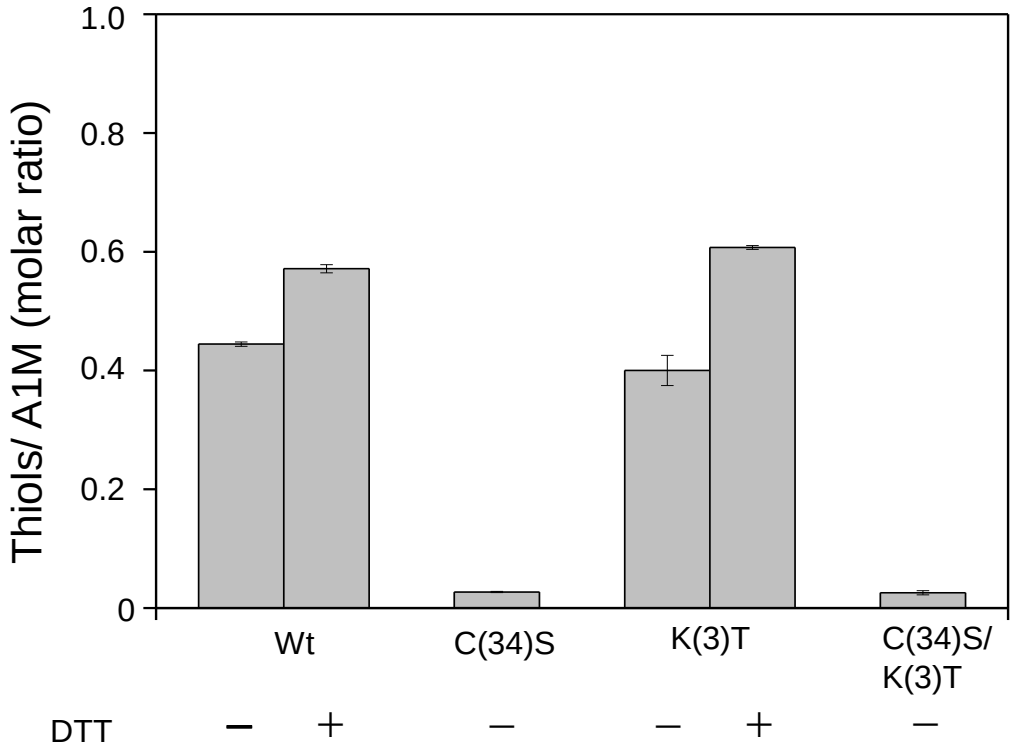

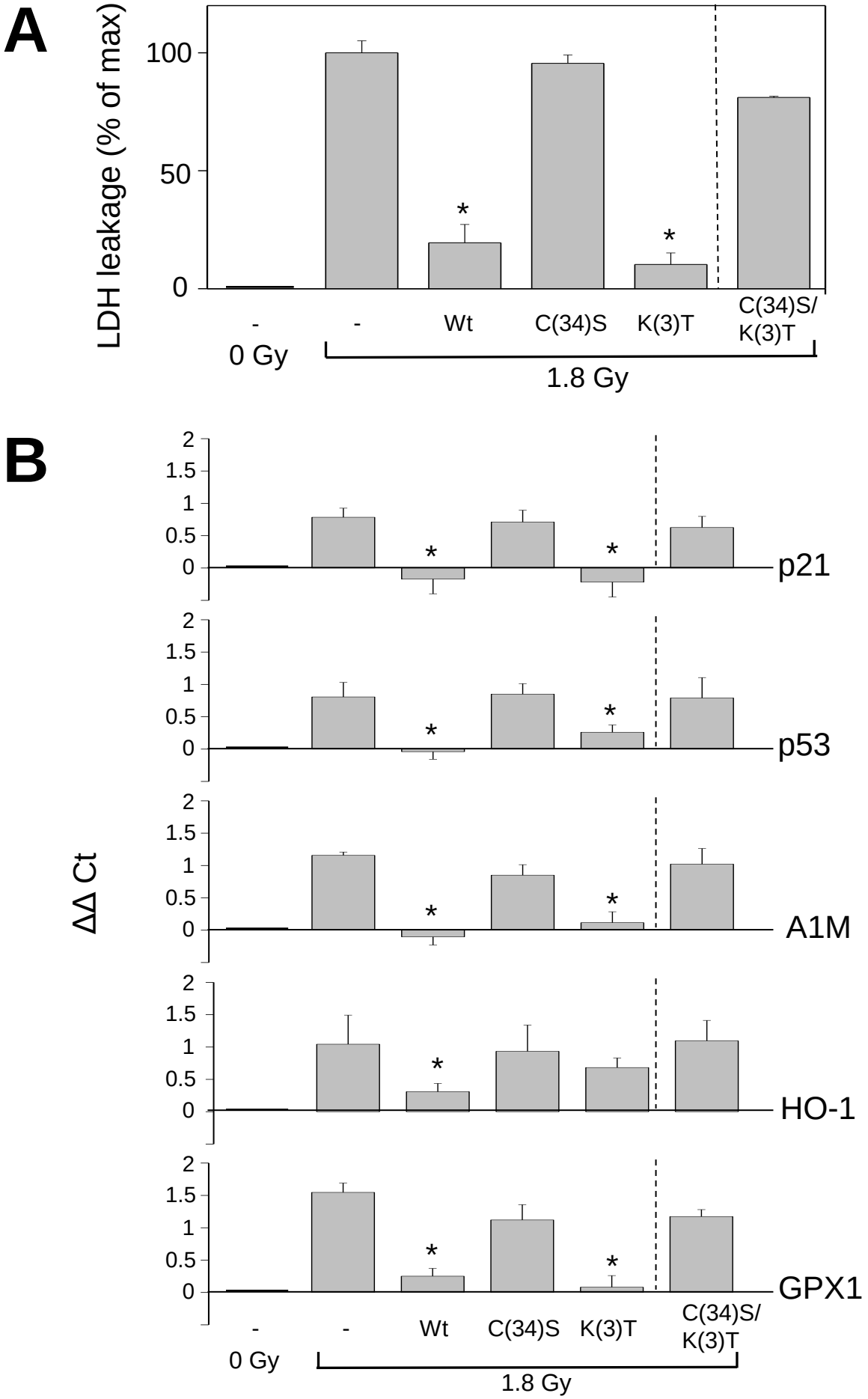
A
LDH leakage (% of max)
100
50
0
*
*
-
-
Wt
C(34)S
K(3)T
C(34)S/
K(3)T
0 Gy
1.8 Gy
B
ΔΔ Ct
2
1.5
1
0.5
0
p21
p53
A1M
HO-1
GPX1
-
-
Wt
C(34)S
K(3)T
C(34)S/
K(3)T
0 Gy
1.8 Gy

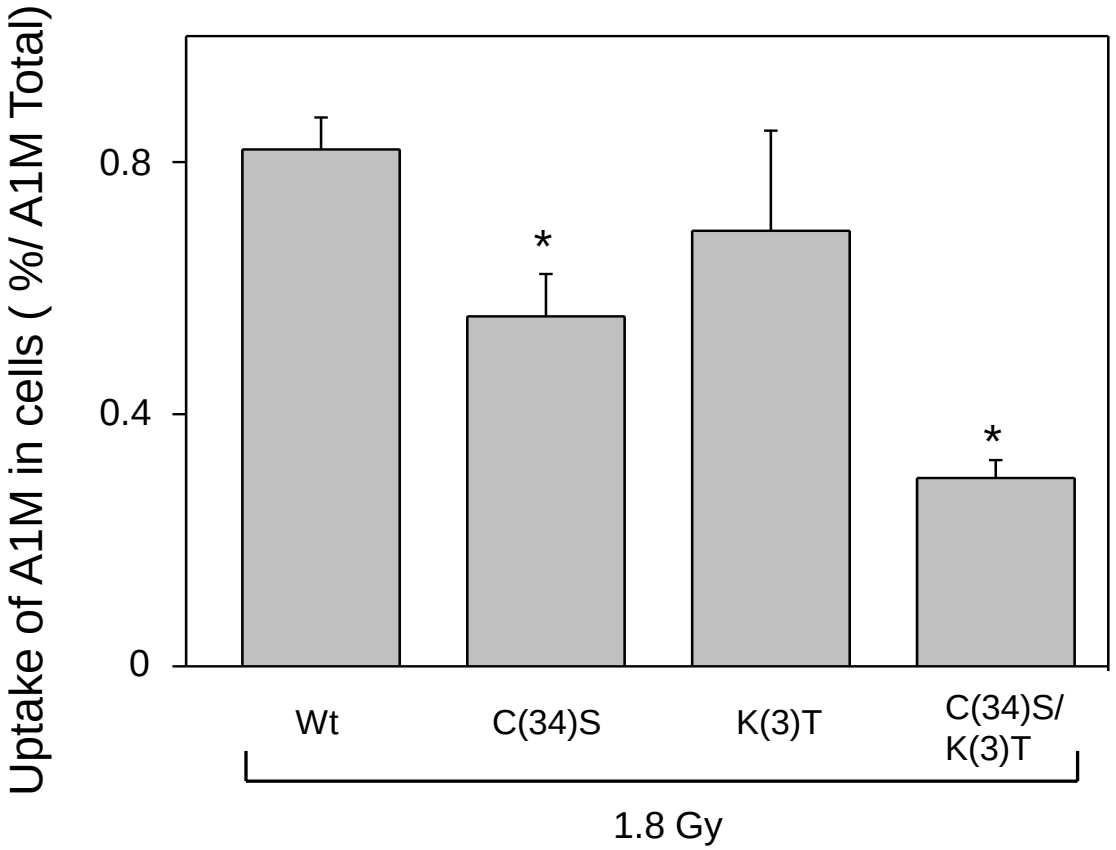
Uptake of A1M in cells (%/ A1M Total)
0.8
0.4
0
*
*
Wt
C(34)S
K(3)T
C(34)S/
K(3)T
1.8 Gy

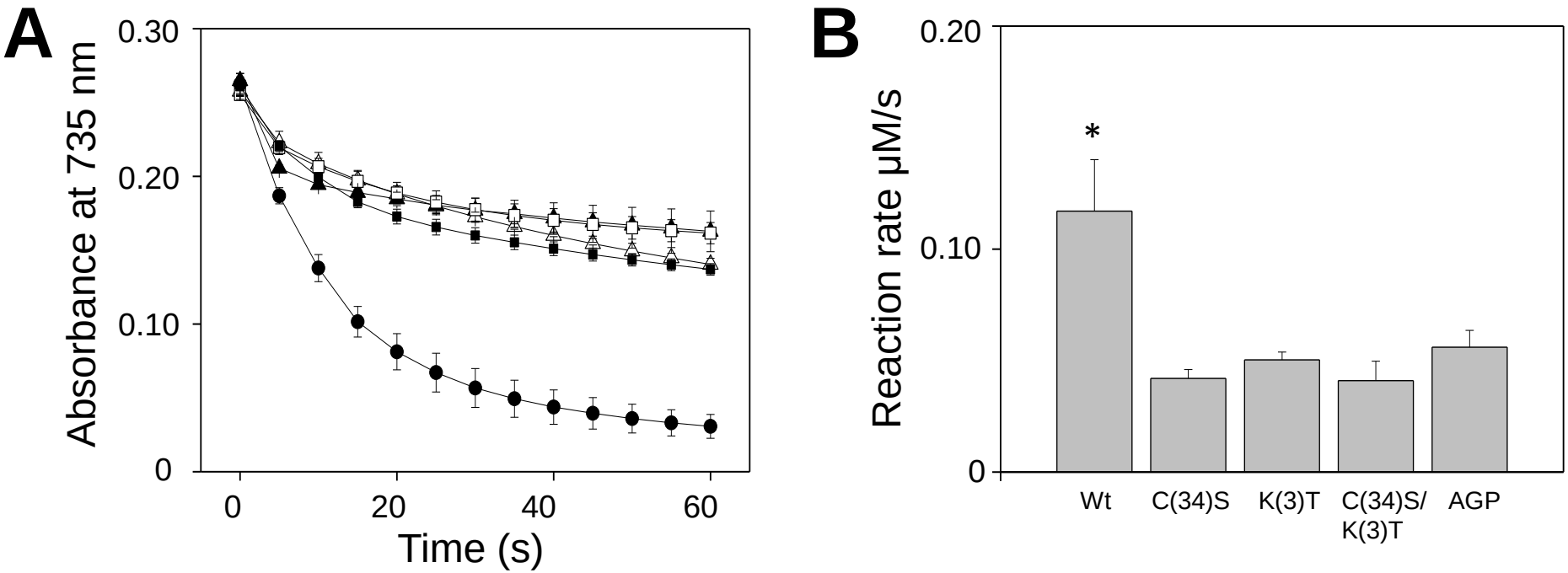
A
Absorbance at 735 nm
0.30
0.20
0.10
0
0
20
40
60
Time (s)
B
Reaction rate µM/s
0.20
0.10
0
*
Wt
C(34)S
K(3)T
C(34)S/
K(3)T
AGP

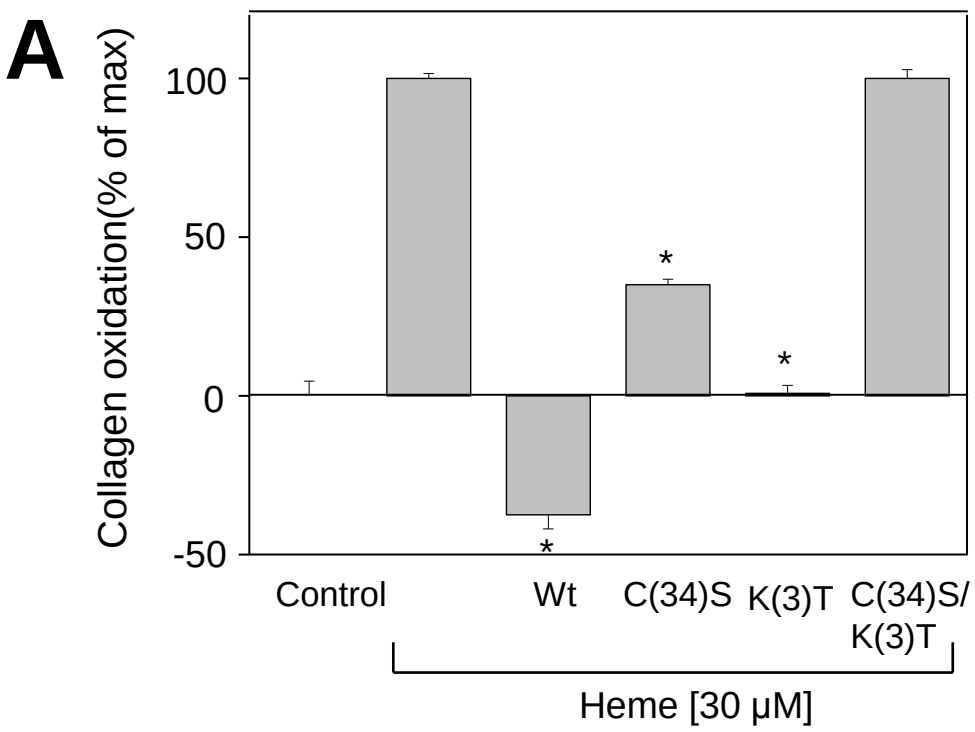
A
Collagen oxidation(% of max)
100
50
0
-50
*
*
*
Control
Wt
C(34)S
K(3)T
C(34)S/
K(3)T
Heme [30 µM]

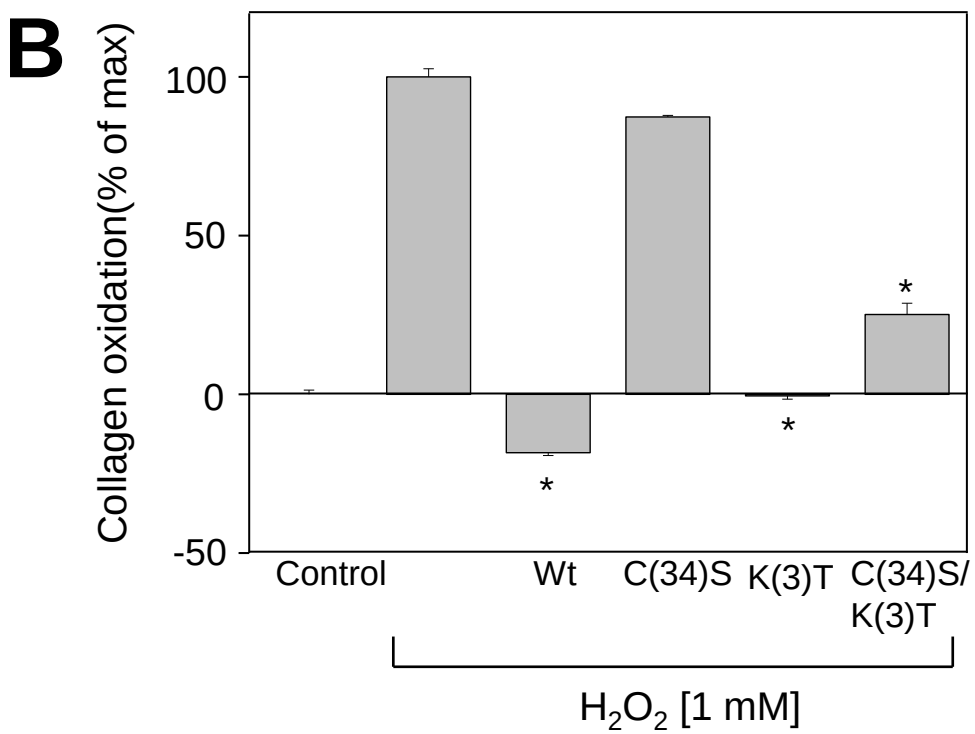
B
Collagen oxidation(% of max)
100
50
0
-50
*
*
*
Control
Wt
C(34)S
K(3)T
C(34)S/
K(3)T
H2O2 [1 mM]